Inorganic Chemistry

Article

Iridium(III) Complexes Formed by O–H and/Or C–H Activation of 2-(Arylazo)phenols

Rama Acharyya,[1a] **Falguni Basuli,**[1a] **Ren-Zhang Wang,**[1b] **Thomas C. W. Mak,**[1b] **and Samaresh Bhattacharya*,**[1a]

Department of Chemistry, Inorganic Chemistry Section, Jadavpur University, Kolkata 700 032, India and Department of Chemistry, The Chinese University of Hong Kong, Shatin, New Territories, Hong Kong

Reaction of 2-(arylazo)phenols with [Ir(PPh₃)₃Cl] in refluxing ethanol in the presence of a base (NEt₃) affords complexes of three different types, viz. [Ir(PPh₃)₂(NO–R)(H)Cl] (R = OCH₃, CH₃, H, Cl and NO₂), [Ir(PPh₃)₂(NO–R)(H)₂] and [Ir(PPh₃)₂(CNO–R)(H)]. Structures of the [Ir(PPh₃)₂(NO–Cl)(H)Cl], [Ir(PPh₃)₂(NO–Cl)(H)₂] and [Ir(PPh₃)₂(CNO–Cl)(H)] complexes have been determined by X-ray crystallography. In the [Ir(PPh₃)₂(NO–R)(H)Cl] and [Ir(PPh₃)₂(NO–R)(H)₂] complexes, the 2-(arylazo)phenolate ligands are coordinated to the metal center as monoanionic bidentate N,O-donors, whereas in the [Ir(PPh₃)₂(CNO–R)(H)] complexes, they are coordinated to iridium as dianionic tridentate C,N,O-donors. In all three products formed in ethanol, the two PPh₃ ligands are trans. Reaction of 2-(arylazo)phenols with [Ir(PPh₃)₃Cl] in refluxing toluene in the presence of NEt₃ affords complexes of two types, viz. [Ir(PPh₃)₂(CNO–R)(H)] and [Ir(PPh₃)₂(CNO–R)Cl]. Structure of the [Ir(PPh₃)₂(CNO–Cl)Cl] complex has been determined by X-ray crystallography, and the 2-(arylazo)phenolate ligand is coordinated to the metal center as a dianionic tridentate C,N,O-donor and the two PPh₃ ligands are cis. All of the iridium(III) complexes show intense MLCT transitions in the visible region. Cyclic voltammetry shows an Ir(III)–Ir(IV) oxidation on the positive side of SCE and an Ir(III)–Ir(II) reduction on the negative side for all of the products.

Introduction

Though 2-(arylazo)phenols (**1**) usually bind to metal ions as bidentate N,O-donors forming a six-membered chelate ring (**2**),[2] they have also been observed to coordinate metal ions as bidentate N,O-donors forming five-membered chelate ring (**3**).[3] In some cases, C—H activation from an ortho position of the pendant phenyl ring has been observed and the 2-(aryl-azo)phenol derivative ligand serves as a tridentate C,N,O-donor (**4**).[4] In our recent studies on the interaction of 2-(aryl-azo)phenols (**1**), Wilkinson's catalyst (viz. [Rh(PPh₃)₃Cl]) was found to successfully induce C—H activation of the
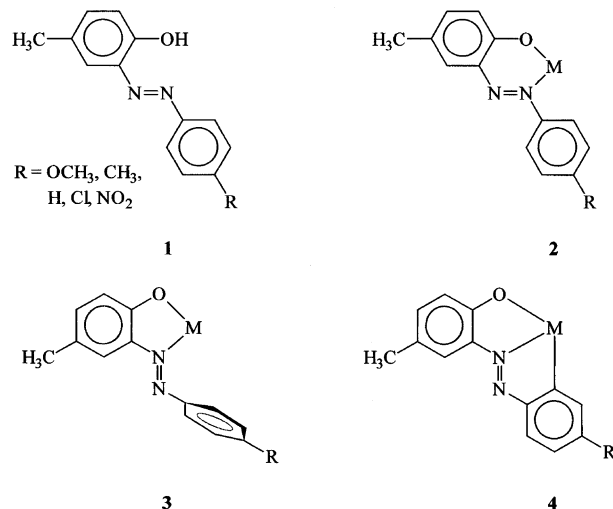
2-(arylazo)phenols. Encouraged by this result, the analogous iridium complex, viz. [Ir(PPh₃)₃Cl], has been chosen to explore further C—H activation of the 2-(arylazo)phenols (**1**). The array of products formed from such reactions is presented herein with special reference to their synthesis and

---

(1) (a) Jadavpur University. (b) The Chinese University of Hong Kong.
(2) (a) Rath, R. K.; Nethaji, M.; Chakravarty, A. R. *J. Organomet. Chem.* **2001**, *633*, 79. (b) Sui, K.; Peng, S. M.; Bhattacharya, S. *Polyhedron* **1999**, *19*, 631. (c) Bhawmik, R.; Biswas, H.; Bandyopadhyay, P. *J. Organomet. Chem.* **1995**, *498*, 81. (d) Sinha, C. R.; Bandyopadhyay, D.; Chakravorty, A. *J. Chem. Soc., Chem. Commun.* **1988**, 468. (e) Dyachenko, O. A.; Atovmyan, L. O.; Aldosin, S. M. *J. Chem. Soc., Chem. Commun.* **1975**, 105. (f) Kalia, K. C. *Indian J. Chem.* **1970**, *8*, 1035. (g) Price, R. J. *J. Chem. Soc. A* **1969**, 1296. (h) Jarvis, J. A. J. *Acta Crystallogr.* **1961**, *14*, 961.
(3) Basuli, F.; Peng, S. M.; Bhattacharya, S. *Polyhedron* **1998**, *18*, 391.

characterization. In this paper, the coordinated 2-(arylazo)-phenolate ligands are in general referred to as NO−R while coordinated as in **3**, and as CNO−R while coordinated as in **4**.

Experimental Section

Materials. Iridium trichloride was obtained from Arora Matthey, Kolkata, India. The para-substituted anilines and *p*-cresol were purchased from S.D., India. The 2-(arylazo)phenols (**1**) were prepared by coupling diazotized para-substituted anilines with *p*-cresol, and [Ir(PPh₃)₃Cl] was prepared by a convenient method developed in our laboratory (see below). Purification of acetonitrile and preparation of tetrabutylammonium perchlorate (TBAP) for electrochemical work were performed as reported in the literature.[5] All other chemicals and solvents were reagent grade commercial materials and were used as received.

Preparations of Complexes. [Ir(PPh₃)₃Cl]. Triphenylphosphine (6 g) was dissolved in hot *tert*-butyl alcohol (200 mL), and the solution was purged with a stream of dinitrogen for 10 min. Iridium trichloride (1 g) was then added to the solution, and it was heated at reflux for 72 h under a dinitrogen atmosphere. [Ir(PPh₃)₃Cl] separated as a yellow crystalline precipitate, which was collected from the hot solution by filtration, washed thoroughly with ether, and dried in air. Yield: 94%.

[Ir(PPh₃)₂(NO─H)(H)Cl], [Ir(PPh₃)₂(NO─H)(H)₂] and [Ir(PPh₃)₂(CNO─H)(H)]. 2-(Phenylazo)-4-methylphenol (25 mg, 0.12 mmol) was dissolved in ethanol (50 mL) and triethylamine (24 mg, 0.24 mmol) was added to it. The solution was then purged with a stream of dinitrogen for 10 min and to it was added [Ir(PPh₃)₃Cl] (100 mg, 0.10 mmol). The mixture was refluxed under a dinitrogen atmosphere for 12 h, whereby a bluish-green solution was obtained. Evaporation of this solution afforded a dark solid, which was subjected to purification by thin-layer chromatography on a silica plate. With benzene as the eluant, three distinct bands (viz. purple, pink and blue) separated, which were extracted separately with acetonitrile. Slow evaporation of the purple, pink, and blue extracts respectively afforded the [Ir(PPh₃)₂(NO−H)-(H)Cl] (yield: 5%), [Ir(PPh₃)₂(NO−H)(H)₂] (yield: 25%), and [Ir(PPh₃)₂(CNO−H)(H)] (yield: 42%) complexes.

Anal. Calcd for [Ir(PPh₃)₂(NO−H)(H)Cl]: C, 61.01; H, 4.36; N, 2.91. Found: C, 61.53; H, 4.37; N, 2.89. ¹H NMR:[6] 7.12−7.43-(2PPh₃); 6.27 (d, 1H, J = 7.9); 6.81 (s, 1H); 6.84−6.98(3H*); 7.00−7.11(3H*); 1.99(CH₃); −20.76(hydride, J = 13.5). Anal. Calcd for [Ir(PPh₃)₂(NO−H)(H)₂]: C, 63.28; H, 4.63; N, 3.01. Found: C, 63.27; H, 4.55; N, 3.09. ¹H NMR: 7.15−7.35(2PPh₃); 6.23 (d, 2H, J = 7.6); 6.44 (d, 1H, J = 8.5); 6.72 (d, 1H, J = 8.7); 6.93 (t, 2H, J = 7.2); 7.06 (s, 1H); 7.12 (t, 1H, J = 7.5); 2.08 (CH₃); −19.16 (hydride, J = 19.5); −23.26 (hydride, J = 15.0). Anal. Calcd for [Ir(PPh₃)₂(CNO−H)(H)]: C, 63.42; H, 4.42; N, 3.02. Found: C, 63.88; H, 4.42; N, 3.09. ¹H NMR: 7.14−7.56(2PPh₃); 6.05 (t, 1H, J = 7.3); 6.23 (d, 1H, J = 8.6); 6.27 (d, 1H, J = 7.6); 6.38 (s, 1H);

(4) (a) Gupta, P.; Butcher, R. J.; Bhattacharya, S. *Inorg. Chem.* **2003**, *42*, 5405. (b) Majumder, K.; Peng, S. M.; Bhattacharya, S. *J. Chem. Soc., Dalton Trans.* **2001**, 284. (c) Dutta, S.; Peng, S. M.; Bhattacharya, S. *J. Chem. Soc., Dalton Trans.* **2000**, 4623. (d) Lahiri, G, K.; Bhatta-charya, S.; Mukherjee, M.; Mukherjee, A, Chakravorty, A. *Inorg. Chem.* **1987**, *26*, 3359.
(5) (a) Sawyer, D. T.; Roberts, J. L., Jr. *Experimental Electrochemistry for Chemists*; Wiley: New York, 1974; pp 167−215. (b) Walter, M.; Ramaley, L. *Anal. Chem.* **1973**, *45*, 165.
(6) Chemical shifts are given in ppm and multiplicity of the signals along with the associated coupling constants(J in Hz) are given in paren-theses. Overlapping signals are marked with an asterisk.

6.49 (d, 1H, J = 8.6); 6.57 (t, 1H, J = 7.4); 7.10 (d, 1H, J = 7.6); 1.91(CH₃); −12.38 (hydride, J = 19.5).

All the other [Ir(PPh₃)₂(NO−R)(H)Cl], [Ir(PPh₃)₂(NO−R)(H)₂], and [Ir(PPh₃)₂(CNO−R)(H)] complexes were prepared by following the same above procedure using appropriate 2-(arylazo)phenols (**1**, R ≠ H) instead of 2-(phenylazo)-4-methylphenol.

Anal. Calcd for [Ir(PPh₃)₂(NO−OCH₃)(H)Cl]: C, 60.38; H, 4.43; N, 2.82. Found: C, 60.07; H, 4.49; N, 2.91. ¹H NMR: 7.15−7.48 (2PPh₃); 6.63 (s, 1H); 6.39−6.50 (4H*); 6.78 (d, 2H, J = 8.3); 1.98 (CH₃); 3.85 (OCH₃); −20.69 (hydride, J = 12.5). Anal. Calcd for [Ir(PPh₃)₂(NO−OCH₃)(H)₂]: C, 62.55; H, 4.69; N, 2.92. Found: C, 61.85; H, 4.37; N, 3.07. ¹H NMR: 7.13−7.43 (2PPh₃); 6.25 (d, 2H, J = 8.0); 6.59 (d, 1H, J = 8.6); 6.92 (d, 1H, J = 8.1); 6.79 (d, 2H, J = 7.8); 7.15 (s, 1H); 2.11 (CH₃); 3.84 (OCH₃); −19.23 (hydride, J = 20.0); −23.19 (hydride, J = 15.5). Anal. Calcd for [Ir(PPh₃)₂(CNO−OCH₃)(H)]: C, 62.68; H, 4.49; N, 2.92. Found: C, 63.19; H, 4.47; N, 2.85. ¹H NMR: 7.16−7.48(2PPh₃); 5.68 (s, 1H); 6.17 (d, 1H, J = 8.5); 6.25 (d, 1H, J = 8.5); 6.37 (s, 1H); 6.47 (d, 1H, J = 8.5); 7.09 (d, 1H, J = 8.5); 1.91 (CH₃); 3.19 (OCH₃); −12.50 (hydride, J = 19.5).

Anal. Calcd for [Ir(PPh₃)₂(NO−CH₃)(H)Cl]: C, 61.37; H, 4.50; N, 2.86. Found: C, 60.85; H, 4.39; N, 2.87. ¹H NMR: 6.92−7.25 (2PPh₃); 6.04 (d, 2H, J = 7.7); 6.44 (s, 1H); 6.50−6.63 (4H*); 1.81 (CH₃); 2.19 (CH₃); −20.97 (hydride, J = 12.0). Anal. Calcd for [Ir(PPh₃)₂(NO−CH₃)(H)₂]: C, 63.61; H, 4.77; N, 2.97. Found: C, 64.01; H, 5.02; N, 2.99. ¹H NMR: 7.11−7.45 (2PPh₃); 6.21 (d, 2H, J = 8.1); 6.44 (d, 1H, J = 8.7); 6.72 (d, 1H, J = 8.9); 6.76 (d, 2H, J = 7.7); 7.02 (s, 1H); 2.08 (CH₃); 2.39 (CH₃); −19.26 (hydride, J = 19.5); −23.22 (hydride, J = 15.0). Anal. Calcd for [Ir(PPh₃)₂(CNO−CH₃)(H)]: C, 63.75; H, 4.57; N, 2.97. Found: C, 63.99; H, 4.51; N, 3.02. ¹H NMR: 7.14−7.50 (2PPh₃); 5.88 (s, 1H); 6.25 (d, 1H, J = 8.6); 6.38 (d, 1H, J = 7.6); 6.40 (s, 1H); 6.48 (d, 1H, J = 7.8); 7.09 (d, 1H, J = 7.9); 1.90 (CH₃); 1.74 (CH₃); −12.53 (hydride, J = 19.5).

Anal. Calcd for [Ir(PPh₃)₂(NO−Cl)(H)Cl]: C, 58.90; H, 4.11; N, 2.80. Found: C, 58.76; H, 4.08; N, 2.81. ¹H NMR: 7.15−7.45-(2PPh₃); 6.24 (d, 1H, J = 8.5); 6.79 (s, 1H); 6.88 (d, 1H, J = 8.6); 7.68 (d, 2H, J = 10.9); 1.98 (CH₃); −20.73 (hydride, J = 12.0). Anal. Calcd for [Ir(PPh₃)₂(NO−Cl)(H)₂]: C, 61.01; H, 4.36; N, 2.91. Found: C, 61.00; H, 4.22; N, 3.04. ¹H NMR: 7.18−7.35 (2PPh₃); 6.19 (d, 2H, J = 8.6); 6.40 (d, 1H, J = 8.7); 6.70 (d, 1H, J = 8.8); 6.86 (d, 2H, J = 8.6); 7.06 (s, 1H); 2.08 (CH₃); −19.15 (hydride, J = 20.0); −23.12 (hydride, J = 15.5). Anal. Calcd for [Ir(PPh₃)₂(CNO−Cl)(H)]: C, 61.14; H, 4.16; N, 2.91. Found: C, 61.59; H, 4.13; N, 2.88. ¹H NMR: 7.15−7.48 (2PPh₃); 6.02 (s, 1H); 6.22 (d, 1H, J = 8.5); 6.41 (s, H); 6.48 (d, 1H, J = 8.7); 6.54 (d, 1H, J = 8.2); 7.07 (d, 1H, J = 8.3); 1.92 (CH₃); −12.44 (hydride, J = 19.5).

Anal. Calcd for [Ir(PPh₃)₂(NO−NO₂)(H)Cl]: C, 58.29; H, 4.06; N, 4.16. Found: C, 58.47; H, 4.07; N, 4.15. ¹H NMR: 7.17−7.47-(2PPh₃); 6.38 (d, 2H, J = 8.9); 6.76 (s, 1H); 6.87 (d, 1H, J = 8.1); 6.98 (d, 1H, J = 9.1); 7.73 (d, 2H, J = 9.2); 2.00 (CH₃); −21.45 (hydride, J = 12.0). Anal. Calcd for [Ir(PPh₃)₂(NO−NO₂)(H)₂]: C, 60.36; H, 4.31; N, 4.31. Found: C, 60.73; H, 4.37; N, 4.29. ¹H NMR: 7.15−7.40 (2PPh₃); 6.24 (d, 2H, J = 8.6); 6.39 (d, 1H, J = 8.8); 6.74 (d, 1H, J = 8.7); 7.13 (s, 1H); 7.70 (d, 2H, J = 9.0); 2.10 (CH₃); −19.00 (hydride, J = 19.5); −23.14 (hydride, J = 15.0). Anal. Calcd for [Ir(PPh₃)₂(CNO−NO₂)(H)]: C, 60.48; H, 4.11; N, 4.32. Found: C, 60.35; H, 4.08; N, 4.29. ¹H NMR: 7.14−7.50 (2PPh₃); 6.24 (d, 1H, J = 8.7); 6.41 (s, 1H); 6.50 (d, 1H, J = 8.7); 6.99 (s, 1H); 7.17 (d, 1H, J = 8.1); 1.91 (CH₃); −12.12 (hydride, J = 19.5).

Table 1. Crystallographic Data for the [Ir(PPh₃)₂(NO−Cl)(H)Cl], [Ir(PPh₃)₂(NO−Cl)(H)₂], [Ir(PPh₃)₂(CNO−Cl)(H)], and [Ir(PPh₃)₂(CNO−Cl)Cl] Complexes

	[Ir(PPh₃)₂(NO−Cl)(H)Cl]	[Ir(PPh₃)₂(NO−Cl)(H)₂] 0.025 CH₃CN	[Ir(PPh₃)₂(CNO−Cl)(H)]	[Ir(PPh₃)₂(CNO−Cl)Cl]
empirical formula	C₄₉H₄₁N₂OP₂Cl₂Ir	C₄₉.₅H₄₂.₇₅N₂.₂₅OP₂ClIr	C₄₉H₄₀N₂OP₂ClIr	C₄₉H₃₉N₂OP₂Cl₂Ir
f_w	998.88	974.70	962.42	996.86
space group	orthorhombic, *Pbca*	triclinic, $P\bar{1}$	triclinic, $P\bar{1}$	monoclinic, *C2/c*
a, Å	19.1548(11)	12.1611(6)	11.9489(14)	25.440(2)
b, Å	19.6711(11)	13.8131(7)	17.659(2)	20.054(2)
c, Å	23.2453(14)	14.9683(8)	21.253(3)	19.425(2)
α, deg	90	104.7540(10)	80.931(3)	90
β, deg	90	98.5050(10)	86.527(3)	112.239(3)
γ, deg	90	113.6240(10)	76.068(3)	90
V, Å³	8758.7(9)	2137.24(19)	4297.0(9)	9172.8(17)
Z	8	2	4	8
λ, Å	0.710 73	0.710 73	0.710 73	0.710 73
cryst size, mm	0.40 × 0.22 × 0.16	0.45 × 0.24 × 0.20	0.42 × 0.30 × 0.14	0.37 × 0.23 × 0.09
T, K	293(2)	293(2)	293(2)	293(2)
μ, mm⁻¹	3.282	3.301	3.282	1.567
R1[a]	0.0398	0.0289	0.0585	0.0638
wR2[b]	0.0765	0.0554	0.0923	0.1666
GOF[c]	0.906	0.979	0.885	0.963

[a] $R1 = \sum ||F_o| - |F_c||/\sum|F_o|$. [b] $wR2 = [\sum\{w(F_o^2 - F_c^2)^2\}/\sum\{w(F_o^2)\}]^{1/2}$. [c] $GOF = [\sum(w(F_o^2 - F_c^2)^2)/(M - N)]^{1/2}$, where M is the number of reflections and N is the number of parameters refined.

[Ir(PPh₃)₂(CNO━H)Cl]. 2-(Phenylazo)-4-methylphenol (25 mg, 0.12 mmol) was dissolved in toluene (50 mL) and triethylamine (24 mg, 0.24 mmol) was added to it. The solution was then purged with a stream of dinitrogen for 10 min, and to it was added [Ir(PPh₃)₃Cl] (100 mg, 0.10 mmol). The mixture was refluxed under a dinitrogen atmosphere for 24 h, whereby a bluish-green solution was obtained. Evaporation of this solution afforded a dark solid, which was purified by thin-layer chromatography on a silica plate. With benzene as the eluant, two bands (viz. blue and green) separated, which were extracted separately with acetonitrile. Upon slow evaporation of the blue and green extracts respectively afforded the [Ir(PPh₃)₂(CNO−H)(H)] (yield: 32%) and [Ir(PPh₃)₂-(CNO−H)Cl] (yield: 35%) complexes. Anal. Calcd for [Ir(PPh₃)₂-(CNO−H)Cl]: C, 61.14; H, 4.16; N, 2.91. Found: C, 61.11; H, 3.86; N, 2.90. ¹H NMR: 6.63−7.35 (2PPh₃); 6.22 (d, 1H, $J = 8.2$); 6.28 (s, 1H); 6.39 (t, 1H, $J = 7.3$); 6.46 (d, 1H, $J = 8.7$); 6.52−6.62 (2H*); 1.74 (CH₃).

All of the other [Ir(PPh₃)₂(CNO−R)Cl] complexes were prepared by following the same above procedure using appropriate 2-(aryl-azo)phenols (**1**, R ≠ H) instead of 2-(phenylazo)-4-methylphenol.

Anal. Calcd for [Ir(PPh₃)₂(CNO−OCH₃)Cl]: C, 60.50; H, 4.24; N, 2.82. Found: C, 60.19; H, 4.22; N, 2.79. ¹H NMR: 6.72−7.47 (2PPh₃); 5.55 (s, 1H); 6.08 (d, 1H, $J = 8.0$); 6.20 (d, 1H, $J = 8.5$); 6.31 (s, 1H); 6.37 (d, 1H, $J = 8.5$); 7.02 (d, 1H, $J = 8.5$); 1.74 (CH₃); 3.22 (OCH₃). Anal. Calcd for [Ir(PPh₃)₂(CNO−CH₃)Cl]: C, 61.49; H, 4.30; N, 2.87. Found: C, 61.73; H, 4.31; N, 2.91. ¹H NMR: 6.79−7.55 (2PPh₃); 5.30 (s, 1H); 5.59 (d, 1H, $J = 8.6$); 6.19 (d, 1H, $J = 7.5$); 6.35 (s, 1H); 6.39 (d, 1H, $J = 7.8$); 7.00 (d, 1H, $J = 7.6$); 1.74 (CH₃); 2.15 (CH₃). Anal. Calcd for [Ir(PPh₃)₂-(CNO−Cl)Cl]: C, 59.02; H, 3.91; N, 2.81. Found: C, 58.89; H, 3.88; N, 2.87. ¹H NMR: 6.83−7.56 (2PPh₃); 6.44 (d, 1H, $J = 8.8$); 6.49 (s, 1H); 6.84 (d, 1H, $J = 9.1$); 6.76 (d, 1H, $J = 7.3$); 7.11 (s, 1H); 1.94 (CH₃). Anal. Calcd for [Ir(PPh₃)₂(CNO−NO₂)Cl]: C, 58.41; H, 3.87; N, 4.17. Found: C, 58.83; H, 3.91; N, 4.20. ¹H NMR: 6.75−7.56 (2PPh₃); 6.43 (d, 1H, $J = 8.7$); 6.49 (s, 1H); 6.70 (d, 1H, $J = 8.8$); 7.61 (d, 1H, $J = 8.6$); 8.15 (s, 1H); 1.94 (CH₃).

Physical Measurements. Microanalyses (C, H, N) were performed using a Heraeus Carlo Erba 1108 elemental analyzer. IR spectra were obtained on a Perkin-Elmer 783 spectrometer with samples prepared as KBr pellets. Electronic spectra were recorded on a JASCO V-570 spectrophotometer. ¹H NMR spectra were recorded in CDCl₃ solution on a Bruker Avance DPX 300 NMR spectrometer using TMS as the internal standard. Electrochemical measurements were made using a CH Instruments model 600A electrochemical analyzer. A platinum disk working electrode, a platinum wire auxiliary electrode, and an aqueous saturated calomel reference electrode (SCE) were used in the cyclic voltammetry experiments. All electrochemical experiments were performed under a dinitrogen atmosphere. All electrochemical data were collected at 298 K and are uncorrected for junction potentials.

X-ray Structure Determinations. Single crystals of the [Ir(PPh₃)₂(NO−Cl)(H)Cl], [Ir(PPh₃)₂(NO−Cl)(H)₂], [Ir(PPh₃)₂-(CNO−Cl)(H)], and [Ir(PPh₃)₂(CNO−Cl)Cl] complexes were obtained by slow evaporation of acetonitrile solutions of the respective complexes. Selected crystal data and data collection parameters are given in Table 1. Data on the crystals of the [Ir(PPh₃)₂-(NO−Cl)(H)Cl], [Ir(PPh₃)₂(NO−Cl)(H)₂], and [Ir(PPh₃)₂(CNO−Cl)(H)] complexes were collected on a Siemens Smart CCD diffractometer using graphite-monochromated Mo Kα radiation ($\lambda = 0.710\ 73$ Å) by ϕ and ω scans. Data on the crystal of the [Ir(PPh₃)₂(CNO−Cl)Cl] complex were collected similarly on a Bruker P4 diffractometer. X-ray data reduction and, structure solution and refinement were done using SHELXS-97 and SHELXL-97 programs.[7] The structure was solved by direct methods.

Results and Discussion

Five 2-(arylazo)phenols (**1**) have been used in the present study, differing in the inductive effect of the substituent R, to observe their influence, if any, on the redox potentials of the complexes. Reaction of each 2-(arylazo)phenol with [Ir(PPh₃)₃Cl] was first carried out in refluxing ethanol in the presence of triethylamine, which afforded a mixture of three complexes with distinctly different colors (viz. purple, pink, and blue). Structure of one representative member of each family, viz. the purple, pink, and blue complexes obtained from the reaction with 2-(4′-chlorophenylazo)-4-methylphenol (**1**, R = Cl), has been determined by X-ray crystallography. The structures are shown in Figures 1−3 and some

(7) Sheldrick, G. M. *SHELXS-97* and *SHELXL-97*, Fortran programs for crystal structure solution and refinement, University of Gottingen: Gottingen, Germany; 1997.

Table 2. Selected Bond Distances and Bond Angles for the
[Ir(PPh₃)₂(NO−Cl)(H)Cl], [Ir(PPh₃)₂(NO−Cl)(H)₂],
[Ir(PPh₃)₂(CNO−Cl)(H)], and [Ir(PPh₃)₂(CNO−Cl)Cl] Complexes

	[Ir(PPh$_3$)$_2$(NO−Cl)(H)Cl]		
	Bond Distances (Å)		
Ir(1)−H(1)	1.42(4)	C(43)−O(1)	1.293(8)
Ir(1)−N(2)	2.029(5)	C(43)−C(44)	1.409(8)
Ir(1)−O(1)	2.149(4)	C(44)−N(2)	1.449(7)
Ir(1)−P(1)	2.3640(17)	N(1)−N(2)	1.248(7)
Ir(1)−P(2)	2.3295(17)	C(38)−N(1)	1.399(8)
Ir(1)−Cl(1)	2.3859(17)		
	Bond Angles (deg)		
H(1)−Ir(1)−O(1)	168(2)	N(2)−Ir(1)−O(1)	81.87(18)
N(2)−Ir(1)−Cl(1)	175.91(15)	H(1)−Ir(1)−Cl(1)	96(2)
P(1)−Ir(1)−P(2)	174.52(6)		
	[Ir(PPh$_3$)$_2$(NO−Cl)(H)$_2$]		
	Bond Distances (Å)		
Ir(1)−H(1)	1.36(3)	C(43)−O(1)	1.299(4)
Ir(1)−H(2)	1.42(3)	C(43)−C(44)	1.420(4)
Ir(1)−N(2)	2.167(2)	C(44)−N(2)	1.404(4)
Ir(1)−O(1)	2.166(2)	C(42)−N(1)	1.401(5)
Ir(1)−P(1)	2.3000(8)	N(1)−N(2)	1.286(3)
Ir(1)−P(2)	2.2906(2)		
	Bond Angles (deg)		
H(1)−Ir(1)−N(2)	174.7(14)	N(2)−Ir(1)−O(1)	77.68(9)
H(2)−Ir(1)−O(1)	172.9(13)	H(1)−Ir(1)−H(2)	75.4(19)
P(1)−Ir(1)−P(2)	164.15(3)		
	[Ir(PPh$_3$)$_2$(CNO−Cl)(H)]		
	Bond Distances (Å)		
Ir(1)−H(1)	1.34(4)	C(37)−C(42)	1.452(12)
Ir(1)−C(37)	2.011(9)	C(42)−N(1)	1.393(11)
Ir(1)−N(2)	2.033(7)	N(1)−N(2)	1.275(9)
Ir(1)−O(1)	2.174(6)	N(2)−C(43)	1.413(11)
Ir(1)−P(1)	2.309(2)	C(44)−O(1)	1.316(10)
Ir(1)−P(2)	2.315(2)		
	Bond Angles (deg)		
H(1)−Ir(1)−N(2)	168(4)	C(37)−Ir(1)−N(2)	77.7(3)
C(37)−Ir(1)−O(1)	157(3)	N(2)−Ir(1)−O(1)	79.3(3)
P(1)−Ir(1)−P(2)	161.86(9)		
	[Ir(PPh$_3$)$_2$(CNO−Cl)Cl]		
	Bond Distances (Å)		
Ir(1)−C(1)	2.044(11)	C(7)−O(1)	1.317(13)
Ir(1)−N(1)	2.026(8)	C(7)−C(8)	1.404(16)
Ir(1)−O(1)	2.177(8)	C(8)−N(1)	1.392(13)
Ir(1)−P(1)	2.351(3)	N(1)−N(2)	1.259(11)
Ir(1)−P(2)	2.305(3)	C(6)−N(2)	1.375(14)
Ir(1)−Cl(1)	2.406(3)	C(1)−C(6)	1.452(14)
	Bond Angles (deg)		
C(1)−Ir(1)−O(1)	158.4(3)	C(1)−Ir(1)−N(1)	79.1(4)
N(1)−Ir(1)−P(1)	166.5(2)	N(1)−Ir(1)−O(1)	79.3(3)
P(2)−Ir(1)−Cl(1)	168.88(10)	P(1)−Ir−P(2)	101.56(10)

relevant bond parameters are listed in Table 2. The structure
of the purple complex (Figure 1) shows that the 2-(arylazo)-
phenol is coordinated to iridium, via loss of the phenolic
proton, as a bidentate N,O-donor forming a five-membered
chelate ring (**3**). Two triphenylphosphines, a hydride, and a
chloride are also coordinated to the metal center. The pur-
ple complexes are therefore formulated in general as
[Ir(PPh₃)₂(NO−R)(H)Cl]. The coordinated 2-(arylazo)phe-
nolate ligand, hydride, and chloride have constituted one
equatorial plane with the metal at the center, where the chlor-
ide is trans to the azo nitrogen and the hydride is trans to
the phenolate oxygen. The PPh₃ ligands have taken up the
remaining two axial positions and hence they are mutually
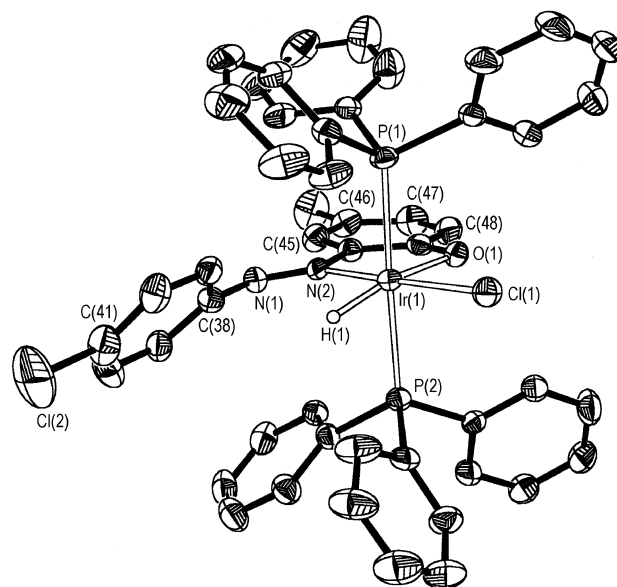
Figure 1. View of the [Ir(PPh₃)₂(NO−Cl)(H)Cl] complex.
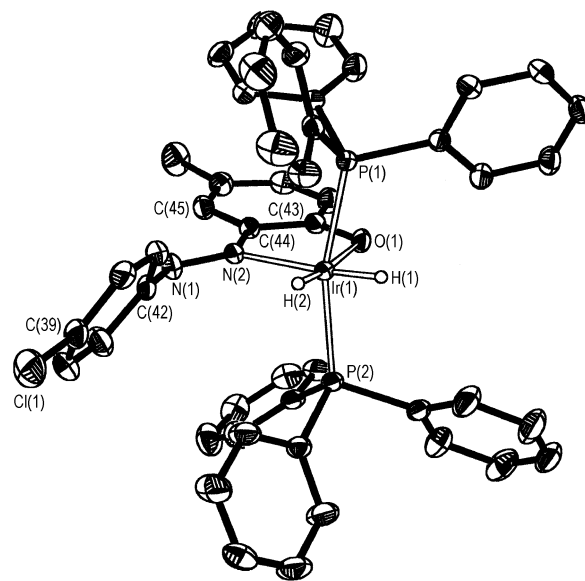
Figure 2. View of the [Ir(PPh₃)₂(NO−Cl)(H)₂] complex.

trans. The Ir−H, Ir−N, Ir−O, Ir−P, and Ir−Cl distances
are all quite normal.[8] The structure of the pink complex (Fig-
ure 2) is very similar to that of the [Ir(PPh₃)₂(NO−Cl)-
(H)Cl] complex, except that a hydride is coordinated to
iridium instead of the chloride, and hence the pink complexes
are generally represented as [Ir(PPh₃)₂(NO−R)(H)₂]. Struc-
ture of the blue complex (Figure 3) shows that the 2-(aryl-
azo)phenol is coordinated to iridium, via loss of two protons,
as a tridentate C,N,O-donor (**4**). Two triphenylphosphines
and a hydride are also coordinated to iridium. The blue
complexes are therefore formulated in general as [Ir(PPh₃)₂-

(8) (a) Canepa, G.; Sola, E.; Martin, M.; Lahoz, F. J.; Ora, L. A.; Werner,
H. *Organometallics* **2003**, *22*, 2151. (b) Lo, K. K. W.; Chung, C. K.;
Ng, D. C. M.; Zhu, N. *New. J. Chem.* **2002**, *26*, 81. (c) Ortmann, D.
A.; Weberndorfer, B.; Ilg, K.; Laubender, M.; Werner, H. *Organo-
metallics* **2002**, *21*, 2369. (d) Torres, F.; Sola, E.; Martin, M.; Ochs,
C.; Picazo, G.; Lopez, J. A.; Lahoz, F. J.; Oro, L. A. *Organometallics*
2001, *20*, 2716. (e) Werner, H.; Heohn, A.; Schulz, M. *J. Chem. Soc.,
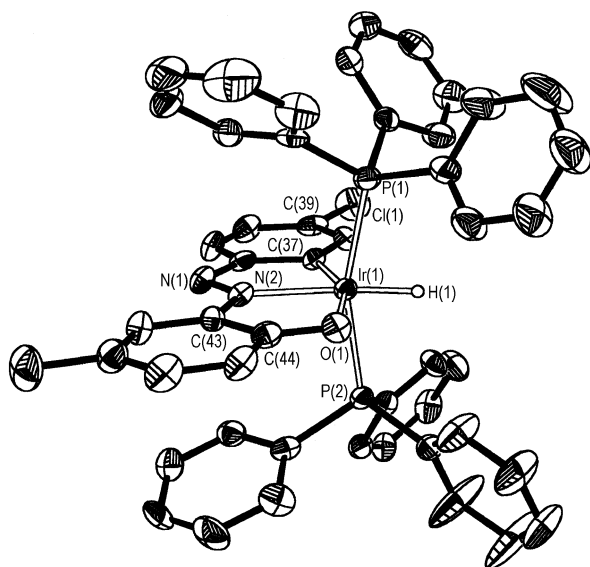Dalton Trans.* **1991**, 777.

Figure 3. View of the [Ir(PPh₃)₂(CNO−Cl)(H)] complex.
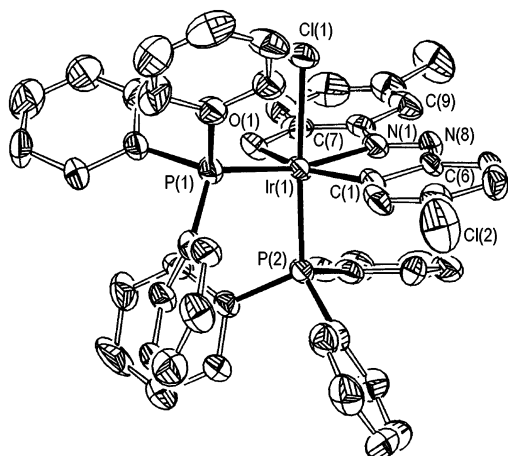
Figure 4. View of the [Ir(PPh₃)₂(CNO−Cl)Cl] complex.

(CNO−R)(H)]. The tricoordinated 2-(arylazo)phenolate ligand is sharing the same equatorial plane with the hydride, and the PPh₃ ligands are trans as before. The Ir−C distance is normal,[8a] and the other bond distances are comparable to those in the previous complexes.

The presence of hydride in all the three types of complexes was quite interesting. Two sources of the hydrides seem probable. Oxidative insertion of iridium(I) into the phenolic O−H bond may generate a hydride, and the solvent (ethanol) may also serve as a source of the hydride. To check this, reaction of each 2-(arylazo)phenol (**1**) with [Ir(PPh₃)₃Cl] was also carried out in a nonalcoholic solvent, viz. toluene, in the presence of triethylamine, which afforded two complexes with different colors, viz. blue and green. Characterization on the blue complexes shows that they are the same [Ir(PPh₃)₂(CNO−R)(H)] complexes obtained from the ethanol reaction, which clearly indicates that ethanol has not been the only source of hydride. Structure determination of a representative green complex, viz. the complex obtained from the reaction with 2-(4′-chlorophenylazo)-4-methylphenol (**1**, R = Cl), shows (Figure 4, Table 2) that the 2-(arylazo)-phenol is again coordinated to iridium as a tridentate C,N,O-

Scheme 1. Probable Steps of the Reaction in Ethanol
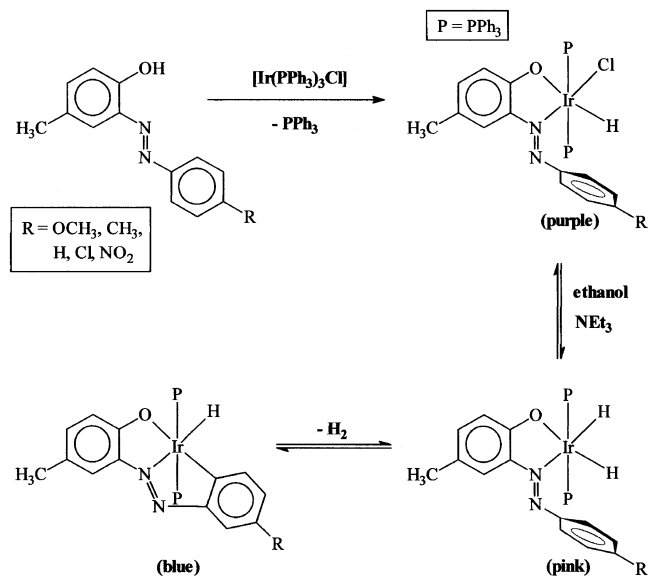
donor (**4**), as in the [Ir(PPh₃)₂(CNO−R)(H)] complexes. Two triphenylphosphines and a chloride are also coordinated to the metal center. Unlike in the previous complexes, the PPh₃ ligands are cis in this complex. The green complexes are therefore represented in general as [Ir(PPh₃)₂(CNO−R)Cl]. Structural features in the Ir(CNO−Cl) fragment of this [Ir(PPh₃)₂(CNO−Cl)Cl] complex compare well with those in the same fragment of the [Ir(PPh₃)₂(CNO−Cl)(H)] complex. The Ir(1)−P(2) bond, which has occupied an axial position, is similar in length with the other axial Ir−P bonds in the previous complexes, while the Ir(1)−P(1) bond, which is sharing the equatorial plane with the 2-(arylazo)-phenolate ligand, is much longer. The Ir(1)−Cl(1) distance is also found to be slightly longer than that observed in [Ir(PPh₃)₂(NO−Cl)(H)Cl].

As all five complexes belonging to each group, viz. [Ir(PPh₃)₂(NO−R)(H)Cl], [Ir(PPh₃)₂(NO−R)(H)₂], [Ir(PPh₃)₂-(CNO−R)(H)], and [Ir(PPh₃)₂(CNO−R)Cl], have been synthesized similarly and they show similar properties (vide infra), the other four members of each group (with R ≠ Cl) are assumed to have structures similar to those of their respective structurally characterized (R = Cl) analogues. The observed microanalytical data of all the complexes agree well with their compositions.

The synthetic reactions carried out in two different solvents show that the nature of products obtained depends on the nature of solvent used. When ethanol is used as the solvent, complexes of three types, viz. [Ir(PPh₃)₂(NO−R)(H)Cl], [Ir(PPh₃)₂(NO−R)(H)₂], and [Ir(PPh₃)₂(CNO−R)(H)], are obtained. The mechanism behind the formation of these three types of complexes is not completely clear to us. However, the sequences shown in Scheme 1 seem probable. In the initial step, the 2-(arylazo)phenol binds to the metal center in [Ir(PPh₃)₃Cl] via oxidative insertion of iridium into the phenolic O−H bond and simultaneous dissociation of one PPh₃, and thus affords [Ir(PPh₃)₂(NO−R)(H)Cl]. There is precedence for such O−H activation by iridium(I) in the

literature.[9] [Ir(PPh$_3$)$_2$(NO−R)(H)Cl] then reacts with ethanol in the presence of NEt$_3$, whereby the coordinated chloride gets displaced by a hydride and thus [Ir(PPh$_3$)$_2$(NO−R)(H)$_2$] is produced. Reports of such displacement reaction are available,[10] and evidence for this displacement reaction comes from the fact that purple ethanolic solution of any [Ir(PPh$_3$)$_2$(NO−R)(H)Cl] complex is observed to convert into the corresponding pink solution of [Ir(PPh$_3$)$_2$(NO−R)(H)$_2$] complex in the presence of NEt$_3$. In the final step, C−H activation at the ortho position of the pendant phenyl ring of the N,O-coordinated 2-(arylazo)phenolate ligand takes place via elimination of molecular hydrogen leading to the formation of [Ir(PPh$_3$)$_2$(CNO−R)(H)]. Similar C−H activation by iridium(III) is well documented in the literature.[11] Such cyclometalation reaction, involving a coordinated hydride close to a pendant phenyl ring, has recently been observed by us.[4a] Evidence for this cyclometalation step also comes from the fact that pink solutions of the [Ir(PPh$_3$)$_2$-(NO−R)(H)$_2$] complexes are observed to gradually transform into blue solutions of the [Ir(PPh$_3$)$_2$(CNO−R)(H)] complexes. The cyclometalated [Ir(PPh$_3$)$_2$(CNO−R)(H)] complex thus appears to be the ultimate product, and the [Ir(PPh$_3$)$_2$-(NO−R)(H)Cl] and [Ir(PPh$_3$)$_2$(NO−R)(H)$_2$] complexes are the intermediates formed under the prevailing reaction conditions. Source of the hydride in the [Ir(PPh$_3$)$_2$(NO−R)-(H)Cl] complexes seems to be the phenolic proton of the 2-(arylazo)phenols, while that of the second hydride in the [Ir(PPh$_3$)$_2$(NO−R)(H)$_2$] complexes appears to be ethanol.

When reaction of the 2-(arylazo)phenols (**1**) with [Ir(PPh$_3$)$_3$Cl] is carried out in toluene, organoiridium complexes of two types, viz. [Ir(PPh$_3$)$_2$(CNO−R)(H)] and [Ir(PPh$_3$)$_2$(CNO−R)Cl], are obtained and the probable steps behind their formation are illustrated in Scheme 2. As before, oxidative addition of 2-(arylazo)phenol to iridium(I) takes place in the first step, yielding two geometric isomers of the [Ir(PPh$_3$)$_2$(NO−R)(H)Cl] complex obtained from the ethanol reaction. These complexes then undergo cyclometalation affording the [Ir(PPh$_3$)$_2$(CNO−R)(H)] and [Ir(PPh$_3$)$_2$-(CNO−R)Cl] complexes via elimination of HCl and H$_2$ respectively. The speculated intermediates could not be isolated in these reactions, probably because they undergo rapid irreversible conversion into the cyclometalated species in refluxing toluene.

Scheme 2. Probable Steps of the Reaction in Toluene
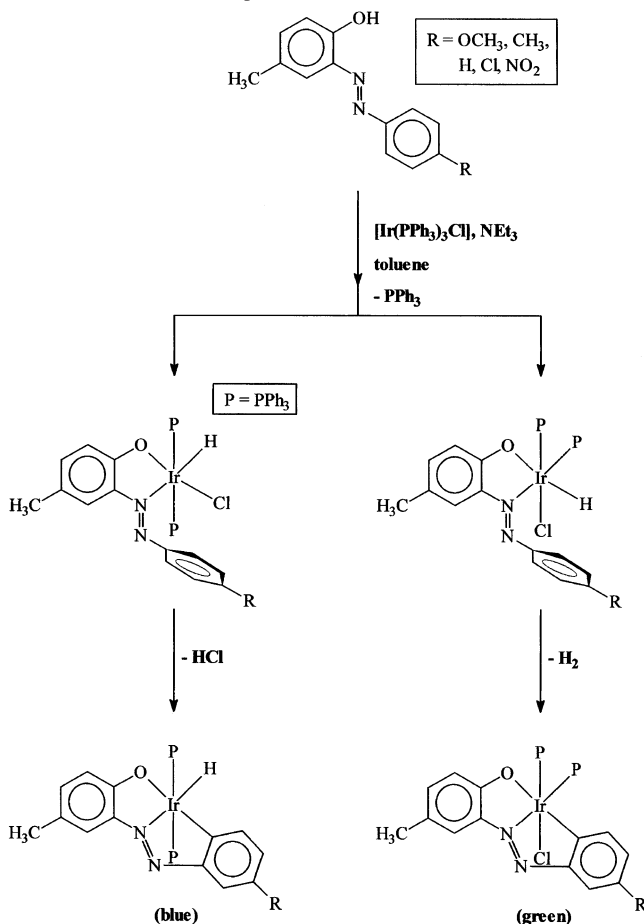
Infrared spectra of the [Ir(PPh$_3$)$_2$(NO−R)(H)Cl], [Ir(PPh$_3$)$_2$-(NO−R)(H)$_2$], and [Ir(PPh$_3$)$_2$(CNO−R)(H)] complexes respectively show one, two, and one strong Ir−H stretch/stretches within 2070−2250 cm^{-1}.[8a,c] Three strong bands near 520, 695, and 745 cm^{-1} are observed in all these complexes due to the coordinated PPh$_3$ ligands.[4,12] Few sharp bands are also displayed by all these complexes within 1200−1400 cm^{-1}, which are absent in the spectrum of [Ir(PPh$_3$)$_3$Cl], and hence these are attributable to the coordinated 2-(arylazo)phenolate ligands. Besides absence of the Ir−H stretch, infrared spectra of the [Ir(PPh$_3$)$_2$(CNO−R)Cl] complexes are mostly similar to those of the [Ir(PPh$_3$)$_2$(CNO−R)(H)] complexes. ^{1}H NMR spectra of the [Ir(PPh$_3$)$_2$(NO−R)(H)Cl] complexes show broad signals within 6.92−7.48 ppm due to the coordinated PPh$_3$ ligands. In each complex, the hydride signal is observed as a distinct triplet, due to coupling with the two magnetically equivalent phosphorus nuclei, near −21.0 ppm. The methyl signal of the NO−R ligand is displayed near 1.9 ppm. Most of the expected aromatic proton signals for the coordinated NO−R ligand have been clearly observed in these complexes, while few signals could not be detected due to their overlap with other signals. Signals

(9) (a) Warner, H.; Papenfubs, B.; Steinert, P. *Z. Anorg. Allg. Chem.* **2001**, *627*, 1807. (b) Dorta, R.; Togni, A. *Organometallics* **1998**, *17*, 3423. (c) Dobbs, D. A.; Bergmann, R. G. *J. Am. Chem. Soc.* **1993**, *115*, 3836. (d) Eberhardt, G. C.; Tadros, M. E.; Vaska, L. *J. Chem. Soc., Chem. Commun.* **1972**, *5*, 290.

(10) (a) Empsall, H. D.; Johnson, S.; Shaw, B. L. *J. Chem. Soc., Dalton Trans.* **1980**, 302. (b) Empsall, H. D.; Hyde, E. M.; Mentzer, E.; Shaw, B. L.; Uttley, M. F. *J. Chem. Soc. A* **1976**, 2069. (c) Chatt, J.; Johnson, N. P.; Shaw, B. L. *J. Chem. Soc. A* **1964**, 1625.

(11) (a) Dorta, R.; Goikhman, R.; Milstein, D. *Organometallics* **2003**, *22*, 2806. (b) Klei, S. R.; Tilley, T. D.; Bergman, R. G. *Organometallics* **2002**, *21*, 4905. (c) Tellers, D. M.; Yung, C. M.; Arndtsen, B. A.; Adamson, D. R.; Bergman, R. G. *J. Am. Chem. Soc.* **2002**, *124*, 1400. (d) Klei, S. R.; Tilley, T. D.; Bergman, R. G. *J. Am. Chem. Soc.* **2000**, *122*, 1816. (e) Sjoevall, S.; Johansson, M.; Andersson, C. *Organometallics* **1999**, *18*, 2198. (f) Niu, S.; Hall, M. B. *J. Am. Chem. Soc.* **1998**, *120*, 6169. (g) Hinderling, C.; Plattner, D. A.; Chen, P. *Angew. Chem.* **1997**, *36*, 243. (h) Luecke, H. F.; Arndtsen, B. A.; Burger, P.; Bergman, R. G. *J. Am. Chem. Soc.* **1996**, *118*, 2517.

(12) (a) Dutta, S.; Basuli, F.; Peng, S. M.; Lee, G. H.; Bhattacharya, S. *New. J. Chem.* **2002**, *26*, 1607. (b) Basuli, F.; Peng, S. M.; Bhattacharya, S. *Inorg. Chem.* **2001**, *40*, 1126. (c) Das, A. K.; Peng, S. M.; Bhattacharya, S. *J. Chem. Soc., Dalton Trans.* **2000**, 181. (d) Dutta, S.; Peng, S. M.; Lee, G. H.; Bhattacharya, S. *Inorg. Chem.* **2000**, *39*, 2231.

Table 3. Electronic Spectral and Cyclic Voltammetric Data of the Complexes

compound	electronic spectral data λ_{max}/nm (ϵ/M^{-1} cm^{-1})[a]	cyclic voltammetric data[b] E, V vs SCE
[Ir(PPh$_3$)$_2$(NO−OCH$_3$)(H)Cl]	554 (7700), 432 (6100),[c] 338 (16000), 262 (53700)[c]	0.91,[d] −1.00[e]
[Ir(PPh$_3$)$_2$(NO−CH$_3$)(H)Cl]	558 (7400), 430 (5500),[c] 346 (13300), 258 (43800)[c]	1.00,[d] −0.83[e]
[Ir(PPh$_3$)$_2$(NO−H)(H)Cl]	552 (8300), 424 (4200),[c] 346 (24100), 256 (50800)[c]	1.11,[d] −0.72[e]
[Ir(PPh$_3$)$_2$(NO−Cl)(H)Cl]	558 (6800), 426 (3900),[c] 342 (10800), 256 (42000)[c]	1.06,[d] −0.72[e]
[Ir(PPh$_3$)$_2$(NO−NO$_2$)(H)Cl]	592 (8100), 352 (13000), 256 (45500)[c]	1.10,[d] −0.87[e]
[Ir(PPh$_3$)$_2$(NO−OCH$_3$)(H)$_2$]	540 (2400), 394 (2400),[c] 334 (4600), 262 (13300)[c]	1.25,[d] 0.72,[d] −0.97[e]
[Ir(PPh$_3$)$_2$(NO−CH$_3$)(H)$_2$]	544 (3100), 396 (3600),[c] 332 (8500), 268 (21300)[c]	1.29,[d] 0.73,[d] −0.91[e]
[Ir(PPh$_3$)$_2$(NO−H)(H)$_2$]	528 (8700), 376 (5000)[c], 328 (10900), 268 (29500)[c]	1.28,[d] 0.91,[d] −0.81[e]
[Ir(PPh$_3$)$_2$(NO−Cl)(H)$_2$]	534 (12100), 376 (8000),[c] 330 (14700), 266 (39400)[c]	1.29,[d] 0.92,[d] −0.82[e]
[Ir(PPh$_3$)$_2$(NO−NO$_2$)(H)$_2$]	556 (8900), 372 (11400),[c] 336 (13500), 264(30800)[c]	1.33,[d] 0.93,[d] −0.98[e]
[Ir(PPh$_3$)$_2$(CNO−OCH$_3$)(H)]	604 (7800), 566 (6900),[c] 456 (1600),[c] 382 (5200),[c] 340 (10200), 258 (24500)[c]	1.02,[d] 0.57 (72), −0.94[e]
[Ir(PPh$_3$)$_2$(CNO−CH$_3$)(H)]	606 (8800), 574 (8100),[c] 466 (1900),[c] 392 (5000),[c] 388 (14500), 266 (35800)[c]	1.09,[d] 0.64 (70), −1.02[e]
[Ir(PPh$_3$)$_2$(CNO−H)(H)]	610 (7400), 576 (7000),[c] 478 (2000),[c] 398 (3900),[c] 336 (13200), 266 (31800)[c]	1.08,[d] 0.68 (78), −1.04
[Ir(PPh$_3$)$_2$(CNO−Cl)(H)]	614 (7700), 582 (7200),[c] 468 (1700),[c] 394 (4000),[c] 340 (12900), 274 (27000)[c]	1.23,[d] 0.72 (80), −1.08[e]
[Ir(PPh$_3$)$_2$(CNO−NO$_2$)(H)]	678 (12200), 638 (11300),[c] 532 (3400),[c] 434 (5300),[c] 364 (19000), 266 (44500)[c]	1.68,[d] 0.88 (78), −0.96[e]
[Ir(PPh$_3$)$_2$(CNO−OCH$_3$)Cl]	660 (4100), 622 (4000),[c] 386 (7400), 338 (7100), 270 (17400)[c]	1.36,[d] 0.79 (80), −1.03[e]
[Ir(PPh$_3$)$_2$(CNO−CH$_3$)Cl]	666 (3900), 632 (3800),[c] 382 (7600), 340 (9200), 270 (26100)[c]	1.27,[d] 0.83 (60), −1.20[e]
[Ir(PPh$_3$)$_2$(CNO−H)Cl]	672 (4800), 636 (4600),[c] 378 (7800),[c] 354 (10500),[c] 338 (9900),[c] 270 (21700)[c]	1.31,[d] 0.89 (64), −1.16[e]
[Ir(PPh$_3$)$_2$(CNO−Cl)Cl]	678 (6500), 640 (6200),[c] 382 (10200),[c] 360 (12100),[c] 342 (11200),[c] 276 (16300)[c]	1.25,[d] 0.94 (94), −1,12[e]
[Ir(PPh$_3$)$_2$(CNO−NO$_2$)Cl]	744 (7500), 692 (7100),[c] 412 (10400),[c] 382 (14100),[c] 270 (20500)[c]	1.48,[d] 1.10 (69), −0.95[e]

[a] In dichloromethane. [b] Solvent, acetonitrile; supporting electrolyte, TBAP; scan rate 50 mV s^{-1}. [c] Shoulder. [d] E_{pa} value. [e] E_{pc} value.

Table 4. Composition of Selected Molecular Orbitals

compounds	contributing fragments	% contribution of fragments to					
		HOMO	HOMO-1	HOMO-2	LUMO	LUMO+1	LUMO+2
[Ir(PPh$_3$)$_2$(CNO−H)(H)]	Ir	82	56	62	12		
	ap-H	9	40	27	81 (N=N, 53)	98	92
[Ir(PPh$_3$)$_2$(NO−H)(H)$_2$]	Ir	89	70	78	9		
	ap-H		23	12	85 (N=N, 64)	96	96
[Ir(PPh$_3$)$_2$(NO−H)(H)Cl]	Ir	90	73	75	10		
	ap-H		20	18	82 (N=N, 63)	96	96
cis-[Ir(PPh$_3$)$_2$(CNO−H)Cl]	Ir	80	64	75	11		
	ap-H	8	26	15	85 (N=N, 51)	97	95

for the hydrogen-containing substituents in the NO−R ligand (R = OCH$_3$ and CH$_3$) are also observed in the expected region. Besides showing two hydride signals (near −19.0 and −23.0 ppm) ^{1}H NMR spectra of the [Ir(PPh$_3$)$_2$(NO−R)(H)$_2$] complexes are similar to those of the [Ir(PPh$_3$)$_2$(NO−R)(H)Cl] complexes. ^{1}H NMR spectra of the [Ir(PPh$_3$)$_2$(CNO−R)(H)] complexes show a hydride signal near −12.0 ppm, while the other spectral features are qualitatively similar to those of the previous complexes. Except for the absence of the hydride signal, ^{1}H NMR spectrum of each [Ir(PPh$_3$)$_2$(CNO−R)Cl] complex is similar to that of its corresponding [Ir(PPh$_3$)$_2$(CNO−R)(H)] complex.

Electronic spectra of all the complexes, recorded in dichloromethane solution, show several intense absorptions in the visible and ultraviolet regions (Table 3). The absorptions in the ultraviolet region are attributable to transitions within the ligand orbitals, and those in the visible region are probably due to metal-to-ligand charge-transfer transition. To have an insight into the nature of the absorptions in the visible region, qualitative EHMO calculations have been performed[13] on computer-generated models of four representative members of the four types of complexes, where

(13) (a) Mealli, C.; Proserpio, D. M. *CACAO* Version 4.0, Firenze, Italy, 1994. (b) Mealli, C.; Proserpio, D. M. *J. Chem. Educ.* **1990**, *67*, 399.
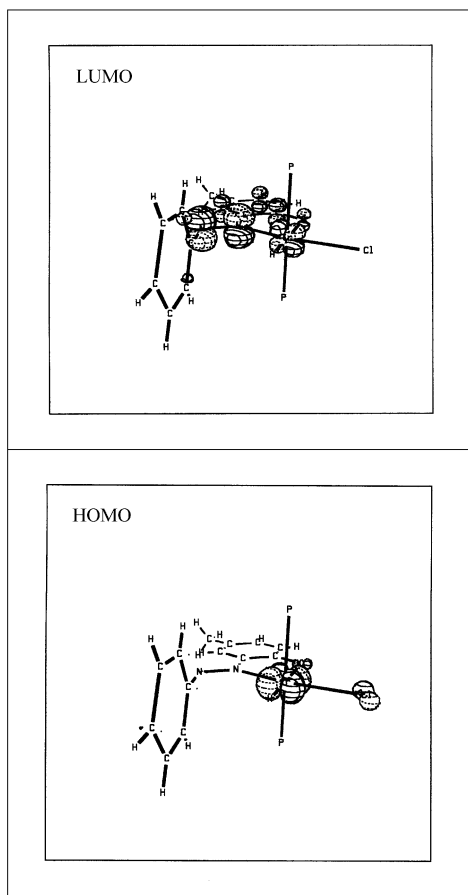
phenyl rings of the triphenylphosphines have been replaced by hydrogens. The results are found to be similar for all the complexes. Compositions of selected molecular orbitals are given in Table 4, and a partial MO diagram of a selected complex is shown in Figure 5. MO diagrams of the other complexes are deposited as Supporting Information (Figures S1−S3). The highest occupied molecular orbital (HOMO) and the next two filled orbitals (HOMO-1 and HOMO-2) have major contribution from the iridium d$_{xy}$, d$_{yz}$, and d$_{zx}$ orbitals. These three occupied orbitals may therefore be regarded as the iridium t$_2$ orbitals. The lowest unoccupied molecular orbital (LUMO) has >80% contribution from the 2-(arylazo)phenolate ligand and is concentrated mostly on the azo (N=N) fragment. The LUMO+1 and LUMO+2 are localized on other parts of the 2-(arylazo)phenolate ligand. The lowest energy absorption in the visible region is therefore assignable to an allowed charge-transfer transition from the filled iridium t$_2$-orbital (HOMO) to the vacant π*(azo)-orbital of the 2-(arylazo)phenolate ligand (LUMO). The other intense absorptions in the visible region may be assigned to charge-transfer transitions from the iridium t$_2$-orbitals to the higher energy vacant orbitals.

Electrochemical properties of all the complexes have been studied by cyclic voltammetry in acetonitrile solution (0.1

Figure 5. Partial molecular orbital diagram of [Ir(PPh$_3$)$_2$(NO$-$H)(H)Cl].

M TBAP). Voltammetric data are given in Table 3. All the complexes show an oxidative response on the positive side of SCE and a reductive response on the negative side, which are respectively assigned to Ir(III)$-$Ir(IV) oxidation and Ir(III)$-$Ir(II) reduction. One-electron stoichiometry of these responses has been established by comparing their current heights with those of standard ferrocene/ferrocenium couple under identical experimental conditions. Except the [Ir(PPh$_3$)$_2$(NO$-$R)(H)Cl] complexes, complexes of the other three types also show a second oxidative response, which is assigned to oxidation of the coordinated 2-(arylazo)phenolate ligand. Cyclic voltammetric behavior of the [Ir(PPh$_3$)$_2$(NO$-$R)(H)$_2$] complexes is similar to that of the [Ir(PPh$_3$)$_2$(NO$-$R)(H)Cl] complexes, except that potential of both Ir(III)$-$Ir(IV) oxidation and Ir(III)$-$Ir(II) reduction is shifted to less positive values. The observed shift is probably due to displacement of the chloride by the hydride. A similar trend is observed within the [Ir(PPh$_3$)$_2$(CNO$-$R)(H)] and [Ir(PPh$_3$)$_2$(CNO$-$R)Cl] series. Except for the Ir(III)$-$Ir(IV) oxidation in the [Ir(PPh$_3$)$_2$(CNO$-$R)(H)] and [Ir(PPh$_3$)$_2$-(CNO$-$R)Cl] complexes, all the redox responses are found to be irreversible in all the complexes. Potential of the irreversible redox responses did not show any systematic

variation with the electron-withdrawing character of the substituent R in the 2-(arylazo)phenolate ligand. However, potential of the reversible Ir(III)$-$Ir(IV) oxidation in the [Ir(PPh$_3$)$_2$(CNO$-$R)(H)] and [Ir(PPh$_3$)$_2$(CNO$-$R)Cl] complexes has been found to be sensitive to the nature of the substituent R. The potential increases with increasing electron-withdrawing character of the substituent R. The plots of oxidation potential vs σ [σ = Hammett constant of R;[14] OCH$_3$ = -0.27, CH$_3$ = -0.17, H = 0.00, Cl = 0.23, and NO$_2$ = 0.78] are linear for both the [Ir(PPh$_3$)$_2$(CNO$-$R)-(H)] and [Ir(PPh$_3$)$_2$(CNO$-$R)Cl] complexes (Figures S4 and S5) with slopes (ρ) of 0.27 and 0.29 V respectively (ρ = reaction constant of this couple[15]), which shows that the para-substituent (R) on the 2-(arylazo)phenolate ligand, which is four bonds away from the metal center, can still influence the metal-centered oxidation potential in a predictable manner.

Conclusions

The present study shows that the 2-(arylazo)phenols (**1**) undergo facile phenolic O$-$H activation and/or C$-$H activation at one ortho position of the phenyl ring in the arylazo fragment, mediated by [Ir(PPh$_3$)$_3$Cl]. Studies on such activation of some other organic molecules, having structural similarity to the 2-(arylazo)phenols, is in progress. Disposition of the Ir$-$H bond in the equatorial plane of the [Ir(PPh$_3$)$_2$(NO$-$R)(H)Cl] complexes (Scheme 1, Figure 1) suggests that C$-$H activation, similar to that observed in the [Ir(PPh$_3$)$_2$(NO$-$R)(H)$_2$] complexes, may also be possible in these complexes under suitable reaction conditions. Such a possibility is currently under exploration.

Supporting Information Available: Partial molecular orbital diagrams of [Ir(PPh$_3$)$_2$(NO$-$H)(H)$_2$] (Figure S1), [Ir(PPh$_3$)$_2$-(CNO$-$H)(H)] (Figure S2) and [Ir(PPh$_3$)$_2$(CNO$-$H)Cl] (Figure S3), least-squares plots of $E_{1/2}$ values of Ir(III)$-$Ir(IV) couple vs σ for the [Ir(PPh$_3$)$_2$(CNO$-$R)(H)] and [Ir(PPh$_3$)$_2$(CNO$-$R)Cl] complexes (Figure S4 and S5), and X-ray crystallographic data in CIF format. This material is available free of charge via the Internet at http://pubs.acs.org.

IC034785W

(14) Hammett, L. P. *Physical Organic Chemistry*, McGraw-Hill: New York, 2nd ed. 1970.
(15) Mukherjee, R. N.; Rajan, O. A.; Chakravorty, A. *Inorg. Chem.* **1982**, *21*, 785.